Stand dynamics modulate water cycling and mortality risk in droughted 1 tropical forest

Stand dynamics modulate water cycling and mortality risk in droughted tropical forest

Antonio C. L. da Costa[1], Lucy Rowland[2*], Rafael S. Oliveira[3], Alex A. R. Oliveira[4], Oliver J. Binks[5], Yann Salmon[6], Steel S. Vasconcelos[7], João A. S. Junior[1], Leandro V. Ferreira[4], Rafael Poyatos[8,9], Maurizio Mencuccini[8,10], Patrick Meir[5,11]

[*]Corresponding Author: l.rowland@exeter.ac.uk (01392 724488)

[1]Instituto de Geosciências, Universidade Federal do Pará, Belém, Brasil

[2]Department of Geography, College of Life and Environmental Sciences, University of Exeter, Exeter, UK.

[3] Instituto de Biologia, UNICAMP, Campinas, Brasil

[4]Museu Paraense Emílio Goeldi, Belém, Brasil

[5] Research School of Biology, Australian National University, Canberra, Australia

[6]Department of Physics, University of Helsinki, Helsinki, Finland

[7] EMBRAPA Amazônia Oriental, Belém, Brasil

[8] CREAF, Campus UAB, Cerdanyola del Vallés 08193, Spain

[9]Laboratory of Plant Ecology, Faculty of Bioscience Engineering, Ghent University, Coupure Links 653, Ghent 9000, Belgium

[10] ICREA, Barcelona, Spain

[11] School of GeoSciences, University of Edinburgh, Edinburgh, UK

Key Words: Tropical Forest, drought, sap flux, transpiration, water cycling, tree mortality

Running title: Tropical forest drought & water cycling

Primary Research Article

Abstract:

Transpiration from the Amazon rainforest generates an essential water source at a global and local scale. However, changes in rainforest function with climate change can disrupt this process, causing significant reductions in precipitation across Amazonia, and potentially at a global scale. We report the only study of forest transpiration following a long-term (>10 year) experimental drought treatment in Amazonian forest. After 15 years of receiving half the normal rainfall, drought-related tree mortality caused total forest transpiration to decrease by 30%. However, the surviving droughted trees maintained or increased transpiration because of reduced competition for water and increased light availability, which is consistent with increased growth rates. Consequently, the amount of water supplied as rainfall reaching the soil and directly recycled as transpiration increased to 100%. This value was 25% greater than for adjacent non-droughted forest. If these drought conditions were accompanied by a modest increase in temperature (e.g. 1.5°C), water demand would exceed supply, making the forest more prone to increased tree mortality.

Introduction

In South America, 25-35% of precipitation is estimated to be recycled via repeated precipitation-evaporation processes as air masses travel west over Amazonian rainforest (Eltahir and Bras, 1994; Zemp et al., 2014). Up to 70% of the water resources of the extensive Rio de La Plata basin are dependent on evapotranspiration from Amazonia (van der Ent et al., 2010). Changes in land cover properties in the Amazon basin can disrupt this recycling process, potentially causing significant reductions in precipitation both in Amazonia and regionally to the La Plata basin (Spracklen et al., 2012), with large economic consequences (Marengo et al., 2016). However, how tropical forest transpiration will respond

to future drought and temperature change remains uncertain. Despite the climatological importance of large gross fluxes of transpiration from the world's tropical rainforests (Lawrence and Vandecar, 2015; Spracklen et al., 2012), predictions of how water recycling from tropical rainforest may change with climate, in particular climate extremes, are poorly constrained by data for this biome (Kume et al., 2011; Restrepo-Coupe et al., 2013). The frequency and intensity of sub-regional extremes in precipitation and temperature are predicted to increase this century, leading to increased drought at seasonal, interannual and decadal timescales (Duffy et al., 2015; Fu et al., 2013). How water use by forests will change remains unclear. Tropical rainforests generally transpire 30-70% of incoming rainfall (Kumagai, 2016), but at their climatic margins, where annual rainfall is 1200-1500 mm/yr (Zelazowski et al., 2011), this value rises to above 90% placing a cap on regional moisture supply, deep soil recharge and river runoff (Kume et al., 2011; van der Ent et al., 2010).

Processes ranging in scale from plant tissue to ecosystem can control how the proportion of rainfall that is recycled changes in response to drought. For individual trees, long-term responses may include physiological changes in water use efficiency, turgor regulation and the sensitivity of xylem hydraulics to cavitation, structural acclimation in new root growth (Eller et al., 2016; Oliveira et al., 2005), or changes in leaf to sapwood or root area ratios (Wolfe et al., 2016). These responses can help regulate gross water demand by the canopy, but ultimately it will be the demographic regulation of stand density via competition for water that will determine whole-system water use and stability (Meir et al. 2015a).

Measurements of sapflux (J_s) are a powerful method to understand the annual and seasonal shifts in forest water use, including the relationship of transpiration to environmental variables (Eller et al., 2015; Fisher et al., 2007; Poyatos et al., 2013) and the physiological plasticity associated with stomatal regulation in trees (Martinez-Vilalta et al., 2014). There are however relatively few reports of continuous sapflux (J_s) measurements in tropical

74 rainforest (Fisher et al., 2007; Granier et al., 1996), none of which have been conducted
75 following long-term drought (>5 years). Studies during long-term drought are essential to
76 establish whether tropical trees can adjust their water use to drier soils over timescales
77 approaching those of possible changes in climate. By imposing a reduction in soil water
78 availability, large scale through-fall exclusion (TFE) provides a unique way to examine the
79 processes underlying long-term responses to increased deficit in soil water potential, and to
80 examine how water use and stand-scale water cycling are altered.

81 Here we quantify the effects of a prolonged experimental soil drought on water use as a
82 proportion of available rainfall by an old-growth tropical rainforest in eastern Amazonia. We
83 use the world's only long-running tropical forest TFE experiment, at the Caxiuanã National
84 Forest Reserve, Pará State, Brazil (da Costa et al., 2010; Meir et al., 2015b; Rowland et al.,
85 2015b), to compare how transpiration and through-fall recycling (the percentage of canopy
86 through-fall transpired by the forest) are altered between a normal forest and a drought-
87 treated forest, with the latter having experienced a 50% TFE treatment since 2002. We
88 previously reported (Rowland et al., 2015a) the loss of about 40% biomass after 14 years
89 since the TFE started. Because measurements of stand scale transpiration were also available
90 for the years 2002-2003, i.e., at the start of the experiment, but before the large waves of
91 mortality occurred, we are also able to determine how total water use and its partitioning
92 changed in response to changes in stand density and structure.

93

94 Materials and Methods

95 Site

96 The site is a long-term through-fall exclusion (TFE) experiment located at the Caxiuanã
97 National Forest Reserve in the eastern Amazon (1°43'S. 51°27W). The site has a mean

rainfall of 2000-2500 mm yr^{-1}, a pronounced dry season between June and November (rainfall <100 mm $month^{-1}$) and is situated on *terra firme* forest, with yellow oxisol soils (Ruivo and Cuhha, 2003).

The TFE experiment consists of two 1 ha plots located on old-growth tropical forest. The treatment plot (TFE) has been covered with plastic panels and guttering 1-2 m in height since 2002. This structure excludes 50% of the incoming canopy through-fall. A control plot, on which no rainfall exclusion has taken place, is located <50 m from the TFE. For further details on the experimental design and results see: da Costa et al., 2010, Meir et al. 2015 and Rowland et al., 2015. Following 14 years of continuous drought the plot has experienced a 40% loss in biomass (equivalent to 100 Mg C ha^{-1}), this loss generated a substantial reduction in basal and thus sapwood area, a reduction in leaf area index (LAI) and an increase in light interception in the lower canopy (see Rowland et al., 2015a).

Meteorological and soil moisture data

All meteorological variables were obtained from a weather station situated at the top of a 40 m tower located in the control forest. During the period of 2014-2016 air temperature, relative humidity, solar radiation and rainfall were monitored half hourly using HC2S3 (Campbell Scientific, Logan, USA), CM3 sensors (Kipp and Zonen, Delft, The Netherlands), and a tipping bucket rain gauge (TE525MM, Campbell Scientific, Logan, USA) respectively. Vapour pressure deficit (VPD) was calculated from temperature and relative humidity. Soil access pits are located in the control and TFE plots. In each soil access pit volumetric soil water content sensors (CS616, Campbell Scientific, Logan, USA) have been placed at depths of 0, 0.5, 1, 2.5 and 4 m, to monitor soil moisture every hour (*cf*. Fisher et al., 2007, for full methodology). Here we use the data collected during 2014-2016, the period during which

sapflux (J_s) data were collected. Hourly relative extractable water (REW) aggregated across the first two meters was calculated using the soil moisture data and following the methodology in Meir et al. 2015. Daily values were calculated using a 30 day running mean so that the seasonal trend of REW was captured, rather than daily or hourly spikes in soil water concentrations.

J_s Data

J_s was measured using the heat balance method (Cermak et al., 1973; Cermak et al., 2004; Kucera et al., 1977) and previously used at the site (Fisher et al., 2007). EMS51 sensors (Environmental monitoring systems; http://www.emsbrno.cz), were used on all trees. The installation process and functioning of these sensors are described in the supplementary information. Between November 2014 and December 2016 the EMS51 sensors were installed on 16 trees in the control plot and 13 trees in the TFE plot. The start date of sampling varied among trees (see Table S1). Trees for which sensors were installed in 2016 (seven on the control and three on the TFE) were excluded from the upscaling analysis (see below) on the basis that they had an insufficient data time series. To ensure we could up-scale with confidence, sensors were strategically placed across trees with a range of diameters at breast height (DBH) values (15-56 cm) and on common species in the control and TFE plots known to be both sensitive and resistant to drought stress (see Table S1).

Values of J_s obtained from the EMS51 sensors were always offset from zero as a constant part of the heat loss from the heated electrodes is conducted into the xylem tissue. To remove this effect the data were baselined, as performed in other standard sap flux processing protocols (e.g. Poyatos et al., 2013). To baseline the data, the minimum value of the J_s for each night was subtracted from all values for the subsequent day, provided evaporative

146 demand was low (preventing night-time J_s, VPD < 0.15 kPa). If night-time VPD > 0.15 kPa,
147 a minimum value was linearly interpolated from the baseline values from surrounding days
148 using the *approx* function in R (R Core team 2014).

149

150 Gapfilling J_s Data

151 Gaps in the data varied from 0% to 63% (average of 8%) and were generally caused by
152 power failure or broken sensors. Gaps in the hourly baselined J_s data since sensor installation
153 were gap-filled using an autoregressive (AR1) style model, accounting for the autocorrelation
154 in the data. Firstly, the *boxcox* function in R was used to determine the lambda value to
155 power transform the J_s data of each tree (lambda range 0.46-0.84). Secondly, a linear
156 regression was performed between the power-transformed J_s, the three independent variables
157 VPD, radiation, REW and six vectors of the power-transformed J_s preceding the dependent
158 variable by one to six hours. We correlated each J_s data point with the six hourly data points
159 preceding it, as this was the number required to remove the autocorrelation effect across all
160 trees (determined using ACF plots). Data from all but one of the trees were gap filled with a
161 model which had an r^2>0.90; the mean model fit was r^2 = 0.93±0.07 (s.e.m.), demonstrating a
162 very good fit between modelled and measured J_s.

163

164 Statistical Analysis

165 All statistical analyses of J_s data were conducted within R 3.0.2 (R Core Team[35]) and all
166 errors are shown as standard deviation. To compare diurnal responses between plots and
167 seasons an average diurnal J_s pattern was calculated for the control and TFE plots, during
168 peak wet and dry season. Peak wet and dry season were determined as the two months with
169 the highest (October and November) and lowest (March and April) monthly average VPD.

Multiple linear regressions between mean daytime transpiration rate per tree, per plot (calculated as the average J_s from all trees per plot) and environmental conditions were fitted to estimate the most important environmental controls on daily J_s. Initially VPD or temperature with radiation, and REW were included in the model and sequentially non-significant variables were excluded in stepwise linear regressions determined by Akaike's information criterion. For the TFE the use of a single model across both wet and dry season was compared to the model fit of using separate wet and dry season models (considering wet season as Feb-Jul and dry season as Aug-Jan). Two models were most effective on the TFE (see Results) and the same seasonal modelling approach was followed with the control plot. The *relaimpo* package in R (Grömping, 2006) was used to calculate the proportion of the explained variance which was accounted for by each variable retained in each of the final models.

Seasonal relationships of VPD to *J*s were created by fitting a sigmoidal function using the SSllogis function in R through average hourly *J*s data for the trees on the control and TFE, binned by VPD classes. Separate relationships were created for peak wet and dry season and the data were normalised using the maximum average *J*s, across plots and seasons, to make the relationships comparable between plots and seasons.

Scaling J_s to calculate plot-scale transpiration and its temperature sensitivity

Scaling J_s from the measured trees for the measured periods to plot level at the yearly time scale involved the following steps in order to properly propagate the sources of uncertainty deriving from tree-to-tree variability in J_s as well as uncertainties in the scaling of J_s with tree DBH.

193 To obtain a scaling relationship between tree J_s and DBH, we regressed J_s data from April-
194 May 2015 (i.e., peak of wet season and when tree DBH were measured) against DBH. This
195 allowed us to additionally included data obtained by Fisher et al. (2007; also collected at peak
196 wet season); all data were obtained using the same measurement method (Environmental
197 monitoring systems; http://www.emsbrno.cz). There was a linear relationship between DBH
198 and mean daytime J_s, with an r^2 of 0.39 and $p<0.01$ (Fig. S1). This scaling relationship was
199 assumed on the control and TFE plot based on similarity of J_s values across the two plots
200 during the wet season (see Results section), and it was applied to the DBH of all trees on both
201 plots measured in 2015 (see Rowland et al. 2015a, for further details). To account for the
202 uncertainty in the parameters of this relationship, 1000 parameter estimates were randomly
203 generated from the model using the covariance matrix for the intercept and slope. These
204 parameters were used to create 1000 estimates of average daytime April and May J_s for all
205 trees >10 cm DBH on both plots. The average daytime J_s values for each tree, for each of the
206 1000 parameter combinations, were then summed to give 1000 plot-scale estimates of
207 transpiration for April and May of the measurement years, accounting for the error on our
208 DBH to J_s relationship. Following this, a second procedure was employed using similar
209 principles to propagate uncertainty from 1,000 estimates of the measured April-May data to
210 the whole year and across the two plots. We employed the best-fit multilinear model per plot,
211 which described how mean daily J_s varies with climate variables (see above). Because of the
212 strong autocorrelation between VPD, RH and air temperature, only the best regressor among
213 these three was finally employed in the upscaling procedure (see supplementary information
214 for further details). Besides the two estimates for the Control and TFE plots, a third estimate
215 of plot-scale transpiration was generated by applying the estimated J_s from the multiple
216 regression models of Control to the standing biomass of TFE. This estimate gives downscaled
217 values of transpiration on Control with the effect of the loss in basal area on the TFE imposed

218 on Control, and the changes in transpiration rates with environmental variables remaining
219 equal to those on Control.

220 To estimate the effects of increasing temperatures on plot scale transpiration, the 1000 model
221 coefficients from above were re-run with temperature, relative humidity and VPD altered
222 according to a 1.5, 2, 3, 4, and 5˚C increases in mean air temperature. We emphasise that the
223 purpose of these temperature rise scenarios is not for future prediction, but to estimate the
224 effects of long-term drought on the sensitivity of the forest to other changes in climate. The
225 scaling procedure was then repeated as above. The transpiration rates at each temperature
226 level were then compared to the canopy through-fall received by each plot assuming a canopy
227 storage term of 21.5% on the control plot, as measured at the site in 2008 (Oliveira et al.,
228 2008; and within the ranges of canopy storage terms measured across other Amazonian
229 forests (Czikowsky and Fitzjarrald, 2009)). On the TFE we scaled down this estimate of
230 canopy storage to 18.1% (Oliveira et al., 2008), in proportion with the leaf area index
231 measured in TFE relative to Control (See Rowland et al., 2015a), assuming that canopy
232 interception decreases proportionally with leaf area. The analysis was also repeated using a
233 canopy storage term of 12% (Czikowsky and Fitzjarrald, 2009) to account for uncertainty in
234 throughfall resulting from differences in LAI across plots (see sensitivity to canopy
235 interception term section). Also we would expect it to provide a lower limit to the sensitivity
236 in TFE because of fewer interception surfaces in TFE (i.e., lower LAI and biomass; Rowland
237 et al., 2015a). However due to an inability to accurately estimate LAI on a per tree basis,
238 which may have changed over time due to the treatment effect and due to the likely increase
239 in atmospheric coupling on the drought relative to the control plot due to increasing mortality
240 over time, we were not able to accurately scale sapflux according to leaf area to estimate
241 differences in leaf level conductance between the plots (e.g. Eller et al., 2015).

242

Results

During the study period (November 2014-December 2016) there were strong seasonal changes in relative extractable water (REW), precipitation and moderate seasonal changes in vapour pressure deficit (VPD) at our study site (Fig. 1). An El Niño event took place across Amazonia in 2015-16, but had limited distinctive influence on climate drivers at our site, which is demonstrated by the El Niño year not creating substantial climate anomalies relative to previous years (Fig. S2). Therefore considering 2015 to represent standard climatological conditions, we find average transpiration is 1389±279 (s.d.) mm yr^{-1} on the control forest plot. On the TFE forest plot a transpiration rate of 964±245 (s.d.) mm yr^{-1} in response to the 50% experimental reduction in throughfall was observed; this represents a 30% decline in transpiration relative to the control. Transpiration therefore comprised 75% (s.d. range = 60-90%) of canopy through-fall on the control, compared to 101% (s.d. range = 75-127%) on the TFE (Fig. 2). These estimates of through-fall recycling at Caxiuanã are similar to the mean values previously quantified at the start of the TFE treatment for the years 2002-3 using updated estimates for canopy interception for the plots (59-71% and 78-103%, control and TFE, respectively, Fig. 2). These estimates are robust to assumptions made regarding the magnitude of canopy rainfall interception as a proportion of total rainfall and to differences in canopy storage caused by different values of leaf area index across plots (see Supplementary Table 2).

Relative to the control, we observed changes in the transpiration rates of trees on the TFE (Fig. 3). However, there was only a 5% difference between 2015 transpiration on the TFE and the transpiration expected if estimates from the control were downscaled to reflect the 40% reduction in biomass and related basal area which occurred between 2002 and 2015 (Fig. 2). This small reduction by low dry season transpiration was countered with higher wet season transpiration on the TFE (Fig.3). Increased seasonality in TFE transpiration meant that

daytime J_s was modelled more effectively using a separate multiple regression model for dry (Aug-Jan) and wet (Feb-Jul) season on the TFE (r^2 dry = 0.60, r^2 wet = 0.69, r^2 whole year = 0.61, all p values <0.01). Dry season variation in transpiration on TFE was explained mostly by REW (44%) and radiation (47%). During the wet season, radiation explained 60% of the variance, VPD 33% and REW 7%. On the control plot air temperature (32%) and radiation (67%) controlled dry season transpiration (r^2=0.81) and radiation (65%) and VPD (35%) were the most important for controlling wet season fluxes (r^2=0.72).

The reduced dry season transpiration flux on the TFE (Fig. 3) was caused by substantially lower peak daytime (11am-4pm) fluxes in the dry season (Fig 4b) compared to the wet season. In contrast, the control plot maintained higher J_s throughout the day in the dry season relative to the wet (Fig. 4a), suggesting low REW constrained J_s during periods of high atmospheric demand on the TFE. The REW constraint resulted in an altered relationship between J_s and VPD in the dry season on the TFE, contrasting with the wet season relationship, which was similar to that observed on the control (Fig. 5). However, this increased seasonality had a limited effect on plot-scale reductions in transpiration relative to the effect of the loss of biomass and related basal area and active sapwood area (Fig. 2 & 3).

Using the multivariate linear models which specified how J_s varied with environmental conditions on the control and TFE plots (see Methods), we explored how transpiration would vary on both plots if an increase in mean temperature of 1.5-5 ˚C and the resultant increases in VPD were imposed, assuming all else remained equal. The increase in absolute transpiration with a 5 ˚C increase in temperature was greater on the control than the TFE, but was proportionally similar (20%, Fig. 6a). However, the TFE would risk exceeding the imposed canopy through-fall supply even at the lowest temperature rise tested (1.5 ˚C, Fig. 6a). In contrast, even with a 5 ˚C rise in temperature, the control forest only reaches a through-fall recycling rate of 91% for transpiration, still below that of the TFE within the

current climate. In addition, both control and TFE recycle >100% of the water they receive between July-December (dry season) under current climate (Fig. 6b), with this value increasing substantially with a 5 ˚C rise in temperature (Fig. 6c). Under the current climate, between July and October the TFE forest transpires more than 6 times the precipitation it receives and this rises to almost 8 times with a 5 ˚C rise in temperature, creating a substantially greater imbalance between transpiration and precipitation (Fig 6b-c).

Discussion

Until now the long-term responses of water use in a tropical forest exposed to soil drought stress have not been studied. With new sapflow data spanning a two-year period we are able to demonstrate that the 40% loss of forest biomass observed on the TFE (Rowland et al 2015a) resulted in a 30% reduction in total forest transpiration. We are also able to demonstrate for the first time that the surviving trees are able to maintain or increase their transpiration rate on a per-tree basis, causing 100% of the available rainfall received by the droughted forest to be used for transpiration. Furthermore we demonstrate that if such drought conditions were combined with a mild temperature rise, further tree mortality would be inevitable, as forest water demand would substantially exceed supply over an annual and multi-annual timescale.

Our estimates of transpiration rates and through-fall recycling rates (Fig. 2, Table S2) are consistent with previous measurements and modelling at this old-growth rainforest site (Carswell et al., 2002; Fisher et al., 2007). They suggest a remarkably constant water flux partitioning over the 15 years of the experiment, despite a substantial shift in forest structure because of high mortality in the TFE-treated plot. The increase in the recycling rate to 100% on the TFE suggests that a high sensitivity by the trees to atmospheric demand for water is maintained even following long-term drought. Our data suggest that drought-induced

317 mortality of the tallest trees changed stand water use patterns, facilitating greater growth
318 competition in the lower canopy, thereby maintaining very high levels of through-fall
319 recycling on the TFE. This is consistent with the observation (Rowland et al. 2015a) that
320 small- and medium-sized trees increased their growth rates after mortality of the taller trees,
321 by responding plastically to increased light availability in the lower canopy. This hypothesis
322 is also consistent with current hydraulic theory, which suggests that trees will continue to
323 compete for, and use up, a limited water supply, provided the advantages accrued from the
324 related carbon gain exceeds the cost of hydraulic damage (Sperry and Love, 2015; Wolf,
325 2016). Plastic reductions in water use as REW declines from wet to dry season on the TFE
326 are likely to only partially alleviate the water stress (Fig. 3 & 4), which would be substantial
327 during climate extremes, and would impose increased tree mortality risk. The intense
328 regrowth by small-to-medium diameter trees (Rowland et al., 2015a) is therefore likely to be
329 the primary driver maintaining through-fall recycling at the high levels seen in 2002-03.

330 Following the mortality of the largest trees, competitive release of small-to-medium diameter
331 trees considerably elevated wet season stem growth on the TFE (Rowland et al., 2015a). As
332 transpiration accompanies photosynthesis and responds to increased radiation availability, it
333 is possible that the TFE trees have acclimated, with elevated water use in the wet season to
334 maximise growth, and restricted growth in the dry season (Figs. 2-3), thus explaining the
335 increased seasonality in transpiration observed on the TFE (Fig. 1). Our sample size prevents
336 us from examining whether sap flux from small-to-medium diameter trees increased relative
337 to large trees. Comparison of sap flux values and canopy through-fall in 2002/03 with those
338 in 2015 provides indirect confirmation of similar levels of competition for water following
339 mortality-related release on TFE. Yearly stand-scale sap flow values on the TFE were
340 estimated as 953 and 805 mm in 2002/03 *vs* 945 mm in 2015 (Table S2). Therefore, despite a
341 40% biomass reduction, water use remained similar over time on a per unit ground area, but

342 increased on a tree-level basis on the TFE, due to having fewer trees per unit ground area.
343 However, we note that our LAI measurements estimate only about a 12-20% reduction in leaf
344 area on the TFE relative to Control (see Rowland et al 2015a), significantly lower than our
345 estimate of a 30% reduction in transpiration. Measurements of LAI in complex multi-layered
346 canopies are notoriously challenging (Breda, 2003) and these difficulties may explain the
347 discrepancy between the two estimates.

348 A shift from radiation and air temperature controlling dry season transpiration on the control
349 plot, to REW and radiation controlling it on the TFE suggests that trees on the TFE adjusted
350 to limit water use during the dry season when REW was low. The strong controlling
351 influence of REW on dry season transpiration on the TFE, but not the control plot suggests
352 low REW restricts dry season transpiration and is most likely linked to significant hydraulic
353 stress as water demand approaches or exceeds supply on seasonal time-scales (Fig. 6).
354 Relative to Control, the TFE forest maintains higher through-fall recycling rates also in the
355 wet season (January to June) when precipitation levels are substantially elevated (Fig 6b-c),
356 resulting in a reduced capacity to recover from dry season water stress. Given predicted
357 changes in VPD, and thus leaf water potential, combined with lower soil water potentials,
358 under some future climate scenarios, there is potential that trees could rapidly be pushed
359 beyond their species-specific hydraulic safety margins (the difference between normally-
360 occurring minimum xylem pressures, and those causing damage to xylem tissues and
361 restricting water transport), potentially causing xylem embolism (Sperry and Love, 2015;
362 Sperry et al., 2016) and/or leaf loss, with the ultimate risk of increased drought-induced
363 mortality. Furthermore, as total annual tropical forest water use approaches total soil water
364 supply, the likelihood of hydraulic damage occurring in the xylem becomes greater. This is
365 particularly the case for large canopy-top trees, which are exposed to greater variability and
366 extremes in VPD, high air temperatures, and larger xylem tensions (Bennett et al., 2015;

367 McDowell and Allen, 2015), which together have been hypothesised to lead to a series of
368 processes causing drought-induced mortality (Anderegg et al., 2016; McDowell and Allen,
369 2015; Mecuccini et al., 2015; Rowland et al., 2015a; Sperry et al., 2016; Wolfe et al., 2016).

370 In future climate scenarios, areas of tropical forest experiencing drought stress are also likely
371 to experience increases in temperature well beyond the moderate levels of 1.5-2 °C
372 (Christensen et al., 2013; Duffy et al., 2015; Fu et al., 2013; Sanderson et al., 2016). Using a
373 novel modelling approach, we demonstrate here that a forest exposed to long term drought is
374 far more likely to have transpiration demand exceed supply than a non-droughted forest (Fig.
375 6). This is driven mostly by transpiration rates exceeding precipitation supply in the dry
376 season by up to eight times in a droughted forest simultaneously experiencing temperature-
377 driven rises in VPD, as would be expected during natural drought. This puts a very large
378 strain on soil water supply, which the non-droughted forest can easily buffer, due to the
379 higher overall wet season recharge of soil water from higher precipitation. Without this re-
380 charge we demonstrate that even a very moderate rise in temperature necessitates tree
381 mortality in order to balance transpiration demand and soil water supply. Although a 50%
382 decline in canopy through-fall on a 10 year time-scale is unlikely within current climate
383 projections, reductions of up to 50% are predicted across parts Amazonia, in a range of recent
384 climate scenario analyses (Christensen et al., 2013, Duffy et al., 2015). This result thus has
385 strong implications for future climate change and carbon cycle feedback predictions, as it
386 suggests that tropical trees will maintain substantial transpiration fluxes even in the face of
387 drought and rising VPD, and that the forest appears to maintain a similar water balance
388 through the process of tree mortality.

389 The overall picture emerging from these results is that compensation processes acting at
390 tissue, tree and stand level have maintained the high levels of through-fall recycling on the
391 TFE-treated forest over more than a decade. While high mortality tended to reduce levels of

competition for water, the mortality-related growth release for small-to-medium sized trees tended to increase it. Additional processes, such as acclimation in leaf:sapwood and leaf:root ratios could also have affected competition for water. Estimated through-fall recycling rates are already at approximately 100% on the TFE after 15 years of reduced soil moisture availability, suggesting that further demands for water can only be facilitated by additional tree mortality. As recycling rates are already >100% in the dry season, even in un-droughted forest, it suggests that rainforest trees must rely on soil (and likely internal) water storage to carry them through to the next wet season, potentially limiting their capacity to maintain carbon uptake, whilst simultaneously also elevating their mortality risk. If the effects of our 50% rainfall reduction, or indeed a similar reduction in basal area imposed by widespread logging, were to occur at a large scale, even the minimum increase in atmospheric temperature which is now deemed unavoidable in the coming century would imply severely reduced deep soil water recharge and runoff, and increased tree mortality risk. The potential implications for regional economies, water supply and climate-carbon cycle feedbacks are substantial.

Acknowledgements

This work is a product of UK NERC grant NE/J011002/1 to PM and MM, CNPQ grant 457914/2013-0/MCTI/CNPq/FNDCT/LBA/ESECAFLOR to ACLD, an ARC grant FT110100457 to PM and a UK NERC independent fellowship grant NE/N014022/1 to LR. It was previously supported by NERC NER/A/S/2002/00487, NERC GR3/11706, EU FP5-Carbonsink and EU FP7-Amazalert to PM. RP acknowledges support of MINECO (Spain), grant CGL2014-5583-JIN. LR would also like to acknowledge the support of Dr. Tim Jupp, University of Exeter, Jiří Kučera EMSBrn, and two anonymous referees

417

418

Figure Captions

Figure 1: Meteorological data for the Caxiuanã site during the sapflux measurement period. In panel (a), precipitation (mm day^{-1}) is shown as grey bars alongside average daily relative extractable water (REW) integrated across three meters soil depth for the control plot continuous black line) and TFE plot (dashed grey line). Panel (b) shows average daily air temperature (°C, grey line) and average daily VPD (kPa, black line).

Figure 2: How transpiration per year (red arrows), canopy through-fall per year (blue arrows) and annual through-fall recycling rate (% circular black arrows) change on the control (a, c) and TFE (indicated by panel structure b, d) plots from 2002-3 (a, b) to 2015 (c, d). The diagram depicts the change in above ground biomass and the shift in forest structure which occurred during the full experimental period because of tree mortality on the TFE.

Figure 3: Daily transpiration (mm day^{-1}) from December 2014 - July 2016 for the control plot (black line), the TFE (dashed black line), and the estimated transpiration flux from the control plot if its values were downscaled to reflect only the effect of basal area loss on the TFE plot (dashed grey line). Grey shaded area shows the standard error on the estimates calculated using a bootstrapping technique (see Methods).

Figure 4: Average diurnal J_s patterns normalised using seasonal maxima per tree during peak wet (March and April, solid black line) and peak dry season (October and November, solid grey line) for trees on control (a.), and TFE (b.). The black dashed line shows the peak wet minus the peak dry season response for each panel and the grey shaded area shows the standard error.

Figure 5: Optimised sigmoidal relationships between J_s and VPD for trees on the control (C, a. & c.) and TFE (b. & d.) plot in peak dry and peak wet season. J_s is binned by VPD and normalised by max hourly J_s per year to make relationships comparable across plots and season.

Figure 6: The effect of increasing temperature on annual transpiration fluxes for control (C) and TFE (a.), under current temperature climate (T, year 2015 used) and under the climate of this year + 1.5, 2, 3, 4, and 5˚C, accounting for temperature-driven changes in relative humidity and vapour pressure deficit. Dashed lines (a.) indicate the rainfall reaching the forest floor on control (black) and TFE (grey). Rainfall reaching the forest floor is estimated from rainfall minus a canopy interception estimate of 21.5% (see Methods). Panel b. and c. show the % of seasonal through-fall recycled as transpiration during the four quarters of the year, under the current climate (b.) and with a 5 °C increase in temperature (c.). Solid lines in b. and c. indicate 100%, where transpiration exceeds the rainfall reaching the soil. Error bars show the standard deviation across the 100 estimates made of each scenario (see Methods).

References

1. Anderegg, W.R.L., Klein, T., Bartlett, M., Sack, L., Pellegrini, A.F.A., Choat, B., Jansen, S. (2016) Meta-analysis reveals that hydraulic traits explain cross-species patterns of drought-induced tree mortality across the globe. Proceedings of the National Academy of Sciences of the United States of America 113, 5024-5029.
2. Bennett, A.C., McDowell, N.G., Allen, C.D., Anderson-Teixeira, K.J. (2015) Larger trees suffer most during drought in forests worldwide. Nature Plants 1.
3. Breda, N.J.J. (2003) Ground-based measurements of leaf area index: a review of methods, instruments and current controversies. Journal of Experimental Botany 54, 2403-2417.
4. Carswell, F.E., Costa, A.L., Palheta, M., Malhi, Y., Meir, P., Costa, J.D.R., Ruivo, M.D., Leal, L.D.M., Costa, J.M.N., Clement, R.J., Grace, J. (2002) Seasonality in CO2 and H2O flux at an eastern Amazonian rain forest. Journal of Geophysical Research-Atmospheres 107.
5. Cermak, J., Deml, M., Penka, M. (1973) New Method of Sap Flow-Rate Determination in Trees. Biologia Plantarum 15, 171-178.

476 6. Cermak, J., Kucera, J., Nadezhdina, N. (2004) Sap flow measurements with some
477 thermodynamic methods, flow integration within trees and scaling up from sample
478 trees to entire forest stands. Trees-Structure and Function 18, 529-546.
479 7. Christensen, J.H., Krishna Kumar, K., Aldrian, E., An, S.I., Cavalcanti, I.F.A., de
480 Castro, M., Dong, W., Goswami, P., Hall, A., Kanyanga, J.K., Kitoh, A., Kossin, Lau,
481 N.C., Renwick, J., Stephenson, D.B., Xie, S.P., Zhou, T., (2013) Climate Phenomena
482 and their Relevance for Future Regional Climate Change. , in: Stocker, T.F., Qin, D. ,
483 Plattner, G.-K., Tignor, M., Allen, S.K., Boschung, J., Nauels, A., Xia, Y., Bex, V.,
484 and Midgley, P.M. (eds.) (Ed.), Climate Change 2013: The Physical Science Basis.
485 Contribution of Working Group I to the Fifth Assessment Report of the
486 Intergovernmental Panel on Climate Change. Cambridge University Press, Cambridge
487 United Kingdom and New York, NY, USA.
488 8. Czikowsky, M.J., Fitzjarrald, D.R. (2009) Detecting rainfall interception in an
489 Amazonian rain forest with eddy flux measurements. Journal of Hydrology 377, 92-
490 105.
491 9. da Costa, A.C.L., Galbraith, D., Almeida, S., Portela, B.T.T., da Costa, M., Silva,
492 J.D., Braga, A.P., de Goncalves, P.H.L., de Oliveira, A.A.R., Fisher, R., Phillips,
493 O.L., Metcalfe, D.B., Levy, P., Meir, P. (2010) Effect of 7 yr of experimental drought
494 on vegetation dynamics and biomass storage of an eastern Amazonian rainforest. New
495 Phytologist 187, 579-591.
496 10. Duffy, P.B., Brando, P., Asner, G.P., Field, C.B. (2015) Projections of future
497 meteorological drought and wet periods in the Amazon. Proceedings of the National
498 Academy of Sciences of the United States of America 112, 13172-13177.

11. Eller, C.B., Burgess, S.S., Oliveira, R.S. (2015) Environmental controls in the water use patterns of a tropical cloud forest tree species, Drimys brasiliensis (Winteraceae). Tree Physiol 35, 387-399.
12. Eller, C.B., Lima, A.L., Oliveira, R.S. (2016) Cloud forest trees with higher foliar water uptake capacity and anisohydric behavior are more vulnerable to drought and climate change. New Phytologist 211, 489-501.
13. Eltahir, E.A.B., Bras, R.L. (1994) Sensitivity of Regional Climate to Deforestation in the Amazon Basin. Advances in Water Resources 17, 101-115.
14. Fisher, R.A., Williams, M., Da Costa, A.L., Malhi, Y., Da Costa, R.F., Almeida, S., Meir, P. (2007) The response of an Eastern Amazonian rain forest to drought stress: results and modelling analyses from a throughfall exclusion experiment. Global Change Biology 13, 2361-2378.
15. Fu, R., Yin, L., Li, W.H., Arias, P.A., Dickinson, R.E., Huang, L., Chakraborty, S., Fernandes, K., Liebmann, B., Fisher, R., Myneni, R.B. (2013) Increased dry-season length over southern Amazonia in recent decades and its implication for future climate projection. Proceedings of the National Academy of Sciences of the United States of America 110, 18110-18115.
16. Granier, A., Biron, P., Breda, N., Pontailler, J.Y., Saugier, B. (1996) Transpiration of trees and forest stands: Short and longterm monitoring using sapflow methods. Global Change Biology 2, 265-274.
17. Grömping, U. (2006) Relative Importance for Linear Regression in R: The Package relaimpo. . Journal of Statistical Software 17, 1-27.
18. Kucera, J., Cermak, J., Penka, M. (1977) Improved Thermal Method of Continual Recording Transpiration Flow-Rate Dynamics. Biologia Plantarum 19, 413-420.

523 19. Kumagai, T., Kanamori, H. and Chappell, N. A., (2016) Tropical forest hydrology. ,
524 Forest Hydrology: Processes, Management and Assessment., Wallingford, UK.
525 20. Kume, T., Tanaka, N., Kuraji, K., Komatsu, H., Yoshifuji, N., Saitoh, T.M., Suzuki,
526 M., Kumagai, T.o. (2011) Ten-year evapotranspiration estimates in a Bornean tropical
527 rainforest. Agricultural and Forest Meteorology 151, 1183-1192.
528 21. Lawrence, D., Vandecar, K. (2015) Effects of tropical deforestation on climate and
529 agriculture (vol 5, pg 27, 2015). Nature Climate Change 5, 174-174.
530 22. Marengo, J.A., Alves, L.M., Torres, R.R. (2016) Regional climate change scenarios in
531 the Brazilian Pantanal watershed. Climate Research 68, 201-213.
532 23. Martinez-Vilalta, J., Poyatos, R., Aguade, D., Retana, J., Mencuccini, M. (2014) A
533 new look at water transport regulation in plants. New Phytol 204, 105-115.
534 24. McDowell, N.G., Allen, C.D. (2015) Darcy's law predicts widespread forest mortality
535 under climate warming. Nature Climate Change 5, 669-672.
536 25. Meir, P., Wood, T.E., Galbraith, D.R., Brando, P.M., Da Costa, A.C.L., Rowland, L.,
537 Ferreira, L.V. (2015a) Threshold Responses to Soil Moisture Deficit by Trees and
538 Soil in Tropical Rain Forests: Insights from Field Experiments. Bioscience 65, 882-
539 892.
540 26. Meir P, Mencuccini M, Dewar RC (2015b). Drought-related tree mortality –
541 addressing the gaps in understanding and prediction. *New Phytologist*, 207, 28-33.
542 27. Mencuccini, M., Miniunno, F., Salmon, Y., Martinez-Vilalta, J., Hölttä, T., (2015)
543 Coordination of physiological traits involved in drought-induced mortality of woody
544 plants. *New Phytologist,* 208, 396-409.
545 28. Oliveira, L.L., Da Costa, R. F., Da Costa, A. C. L., Sousa, F. A. S., Braga, A. P.
546 (2008) Modelagem da Interceptacao na florests nationcal de Caxiuana, no leste da
547 Amazonia Revista Brasileira de Meteorologia 23, 318-326.

548 29. Oliveira, R.S., Dawson, T.E., Burgess, S.S.O., Nepstad, D.C. (2005) Hydraulic
549 redistribution in three Amazonian trees. Oecologia 145, 354-363.
550 30. Poyatos, R., Aguade, D., Galiano, L., Mencuccini, M., Martinez-Vilalta, J. (2013)
551 Drought-induced defoliation and long periods of near-zero gas exchange play a key
552 role in accentuating metabolic decline of Scots pine. New Phytol 200, 388-401.
553 31. Restrepo-Coupe, N., da Rocha, H.R., Hutyra, L.R., da Araujo, A.C., Borma, L.S.,
554 Christoffersen, B., Cabral, O.M.R., de Camargo, P.B., Cardoso, F.L., da Costa,
555 A.C.L., Fitzjarrald, D.R., Goulden, M.L., Kruijt, B., Maia, J.M.F., Malhi, Y.S.,
556 Manzi, A.O., Miller, S.D., Nobre, A.D., von Randow, C., Sa, L.D.A., Sakai, R.K.,
557 Tota, J., Wofsy, S.C., Zanchi, F.B., Saleska, S.R. (2013) What drives the seasonality
558 of photosynthesis across the Amazon basin? A cross-site analysis of eddy flux tower
559 measurements from the Brasil flux network. Agricultural and Forest Meteorology
560 182, 128-144.
561 32. Rowland, L., da Costa, A.C.L., Galbraith, D.R., Oliveira, R.S., Binks, O.J., Oliveira,
562 A.A.R., Pullen, A.M., Doughty, C.E., Metcalfe, D.B., Vasconcelos, S.S., Ferreira,
563 L.V., Malhi, Y., Grace, J., Mencuccini, M., Meir, P. (2015a) Death from drought in
564 tropical forests is triggered by hydraulics not carbon starvation. Nature 528, 119-122.
565 33. Rowland, L., Lobo-do-Vale, R.L., Christoffersen, B.O., Melem, E.A., Kruijt, B.,
566 Vasconcelos, S.S., Domingues, T., Binks, O.J., Oliveira, A.A.R., Metcalfe, D., da
567 Costa, A.C.L., Mencuccini, M., Meir, P. (2015b) After more than a decade of soil
568 moisture deficit, tropical rainforest trees maintain photosynthetic capacity, despite
569 increased leaf respiration. Global Change Biology 21, 4662-4672.
570 34. Ruivo M, E., C., (2003) Mineral and organic components in archaeological black
571 earth and yellow latosol in Caxiuanã, Amazon, Brazil., in: Tiezzi, E., Brebbia, C. A.,

572 Uso, J. L., (eds) (Ed.), Ecosystems and sustainable development. WIT Press,
573 Southampton, UK, pp. 1113–1121.
574 35. Sanderson, B.M., O'Neill, B.C., Tebaldi, C. (2016) What would it take to achieve the
575 Paris temperature targets? Geophysical Research Letters 43, 7133-7142.
576 36. Sperry, J.S., Love, D.M. (2015) What plant hydraulics can tell us about responses to
577 climate-change droughts. New Phytologist 207, 14-27.
578 37. Sperry, J.S., Wang, Y., Wolfe, B.T., Mackay, D.S., Anderegg, W.R.L., McDowell,
579 N.G., Pockman, W.T. (2016) Pragmatic hydraulic theory predicts stomatal responses
580 to climatic water deficits. New Phytologist 212, 577-589.
581 38. Spracklen, D.V., Arnold, S.R., Taylor, C.M. (2012) Observations of increased tropical
582 rainfall preceded by air passage over forests. Nature 489, 282-U127.
583 39. Team, R.C. (2014) R: A Language and Environment for Statistical Computing, R
584 Foundation for Statistical Computing, Vienna,Austria.
585 40. van der Ent, R.J., Savenije, H.H.G., Schaefli, B., Steele-Dunne, S.C. (2010) Origin
586 and fate of atmospheric moisture over continents. Water Resources Research 46.
587 41. Wolf, A., W.R.L. Anderegg, S.W. Pacala (2016) Optimal stomatal behavior with
588 competition for water and risk of hydraulic impairment. . Proceedings of the National
589 Academy of Sciences.
590 42. Wolfe, B.T., Sperry, J.S., Kursar, T.A. (2016) Does leaf shedding protect stems from
591 cavitation during seasonal droughts? A test of the hydraulic fuse hypothesis. New
592 Phytologist, n/a-n/a.
593 43. Zelazowski, P., Malhi, Y., Huntingford, C., Sitch, S., Fisher, J.B. (2011) Changes in
594 the potential distribution of humid tropical forests on a warmer planet. Philosophical
595 Transactions of the Royal Society a-Mathematical Physical and Engineering Sciences
596 369, 137-160.

44. Zemp, D.C., Schleussner, C.F., Barbosa, H.M.J., van der Ent, R.J., Donges, J.F., Heinke, J., Sampaio, G., Rammig, A. (2014) On the importance of cascading moisture recycling in South America. Atmospheric Chemistry and Physics 14, 13337-13359.

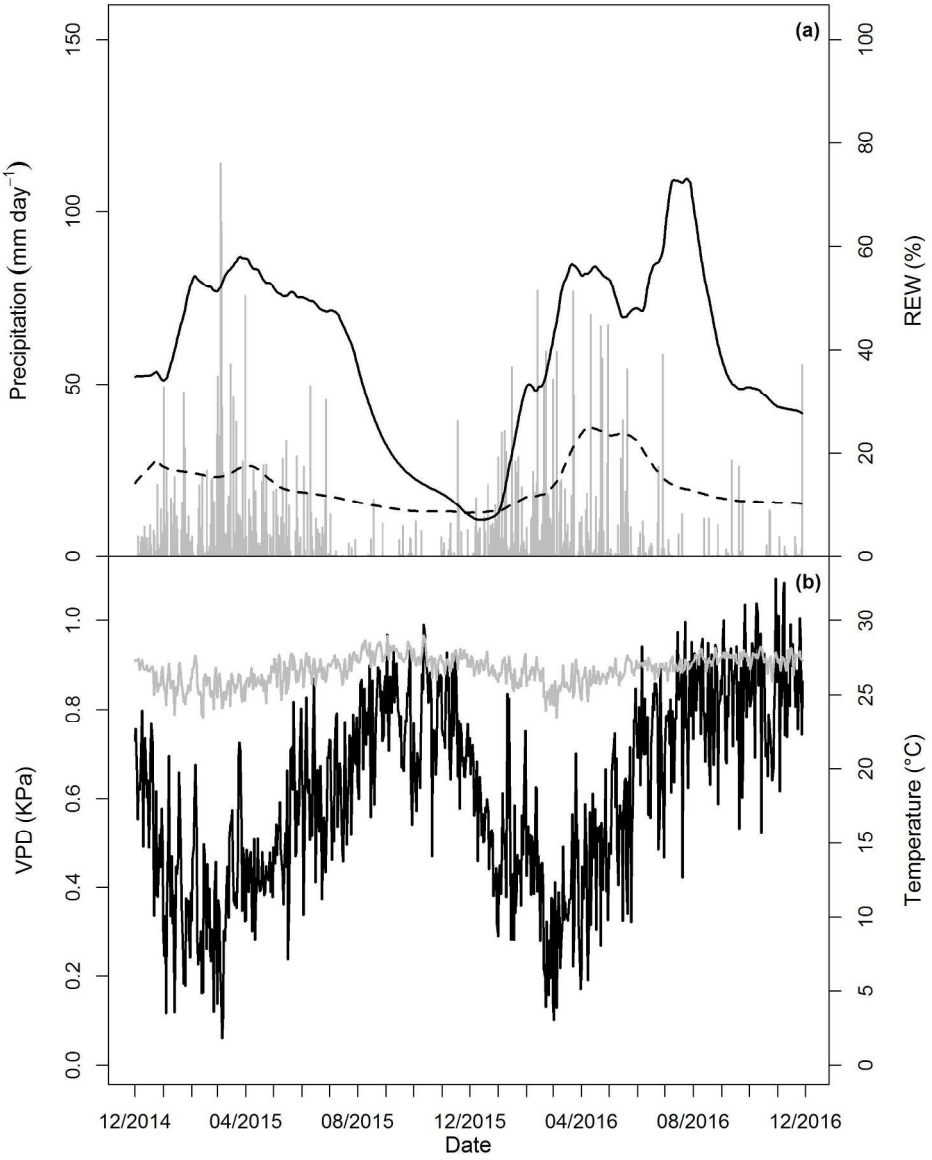

Figure 1: Meteorological data for the Caxiuanã site during the sapflux measurement period. In panel (a), precipitation (mm day-1) is shown as grey bars alongside average daily relative extractable water (REW) integrated across three meters soil depth for the control plot continuous black line) and TFE plot (dashed grey line). Panel (b) shows average daily air temperature (°C, grey line) and average daily VPD (kPa, black line).

203x254mm (300 x 300 DPI)

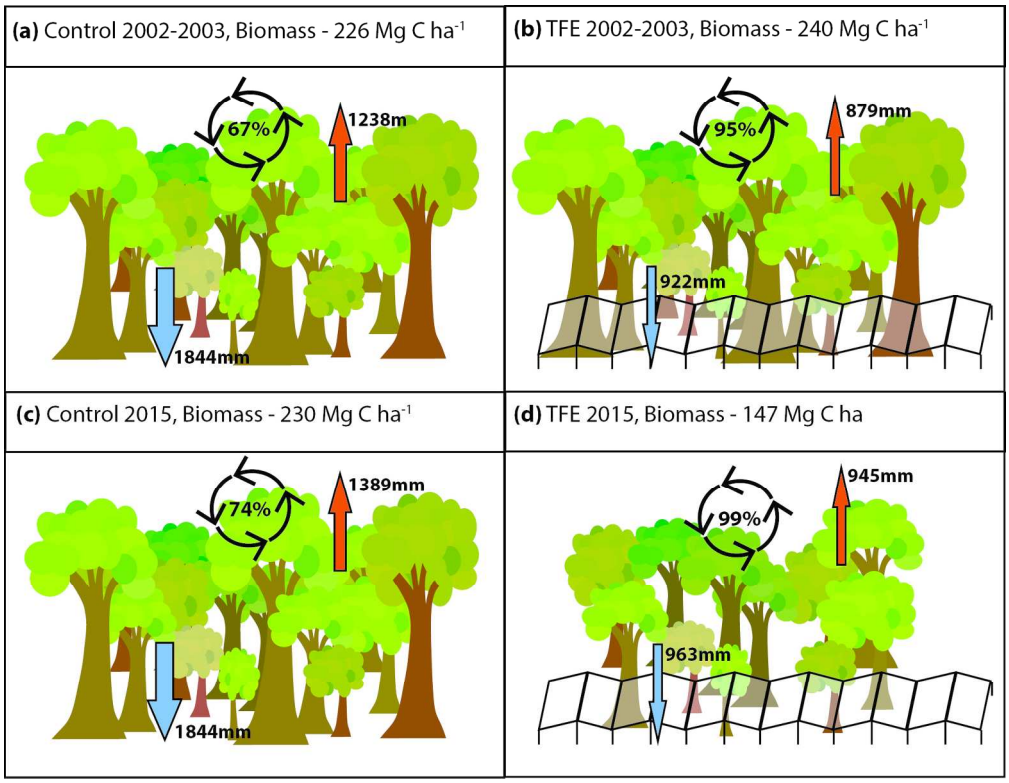

Figure 2: How transpiration per year (red arrows), canopy through-fall per year (blue arrows) and annual through-fall recycling rate (% circular black arrows) change on the control (a, c) and TFE (indicated by panel structure b, d) plots from 2002-3 (a, b) to 2015 (c, d). The diagram depicts the change in above ground biomass and the shift in forest structure which occurred during the full experimental period because of tree mortality on the TFE.

180x139mm (300 x 300 DPI)

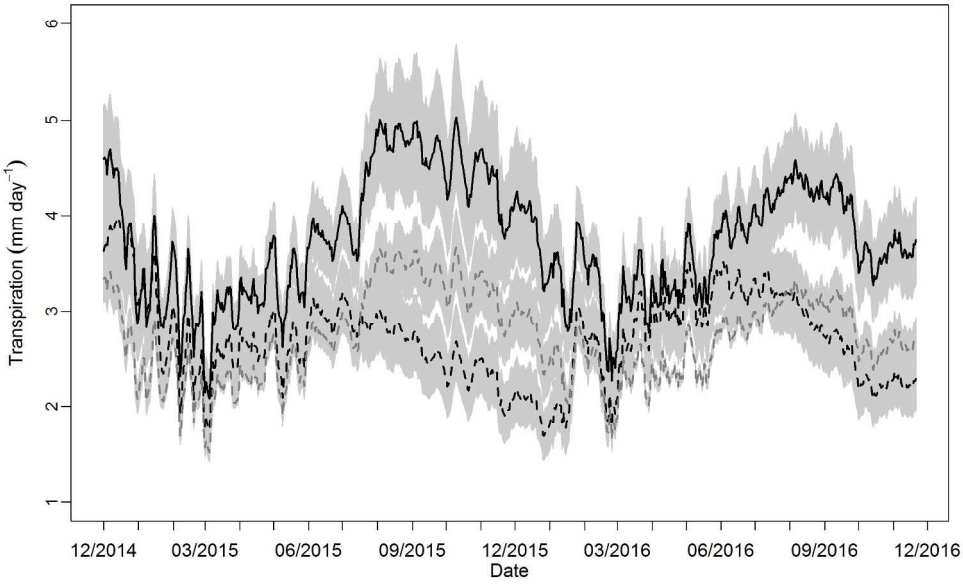

Figure 3: Daily transpiration (mm day-1) from December 2014 - July 2016 for the control plot (black line), the TFE (dashed black line), and the estimated transpiration flux from the control plot if its values were downscaled to reflect only the effect of basal area loss on the TFE plot (dashed grey line). Grey shaded area shows the standard error on the estimates calculated using a bootstrapping technique (see Methods).

254x177mm (300 x 300 DPI)

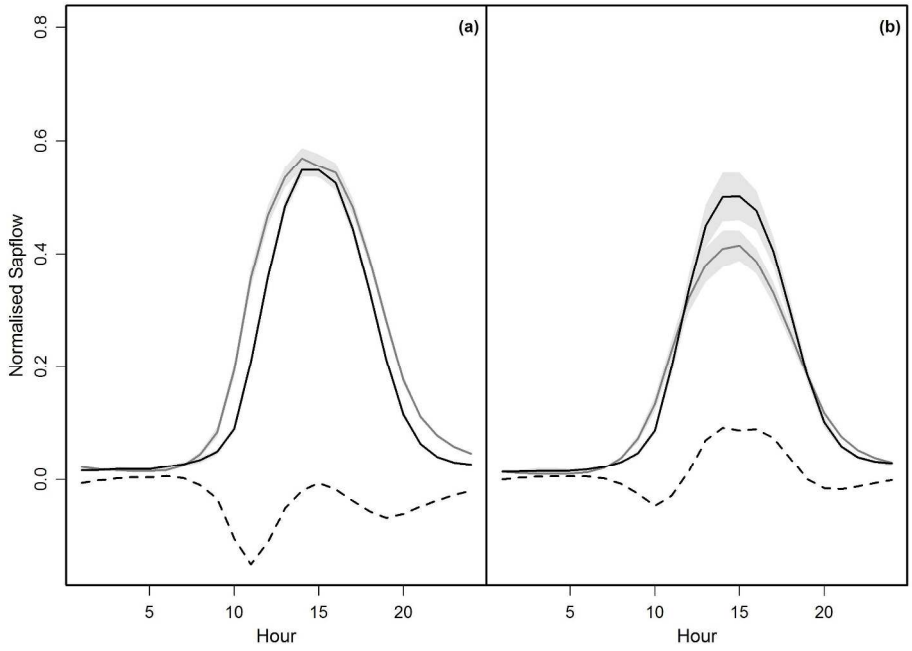

Figure 4: Average diurnal Js patterns normalised using seasonal maxima per tree during peak wet (March and April, solid black line) and peak dry season (October and November, solid grey line) for trees on control (a.), and TFE (b.). The black dashed line shows the peak wet minus the peak dry season response for each panel and the grey shaded area shows the standard error.

254x177mm (300 x 300 DPI)

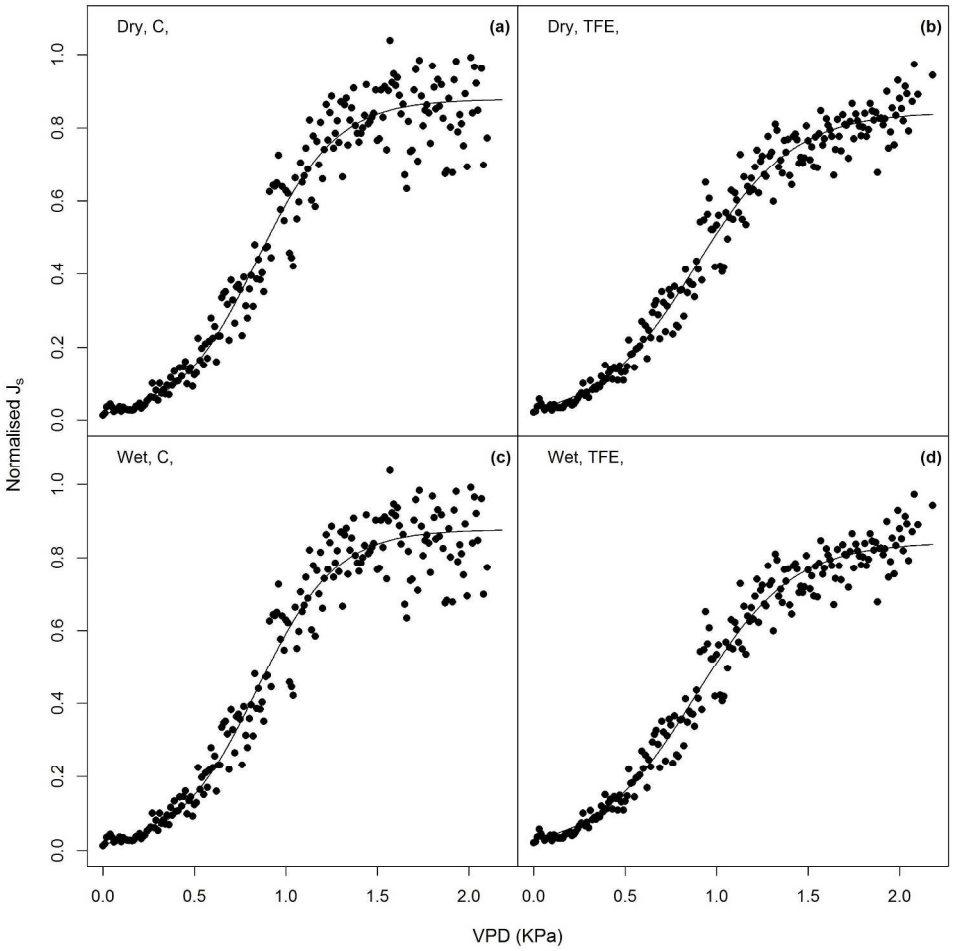

Figure 5: Optimised sigmoidal relationships between Js and VPD for trees on the control (C, a. & c.) and TFE (b. & d.) plot in peak dry and peak wet season. Js is binned by VPD and normalised by max hourly Js per year to make relationships comparable across plots and season.

254x254mm (300 x 300 DPI)

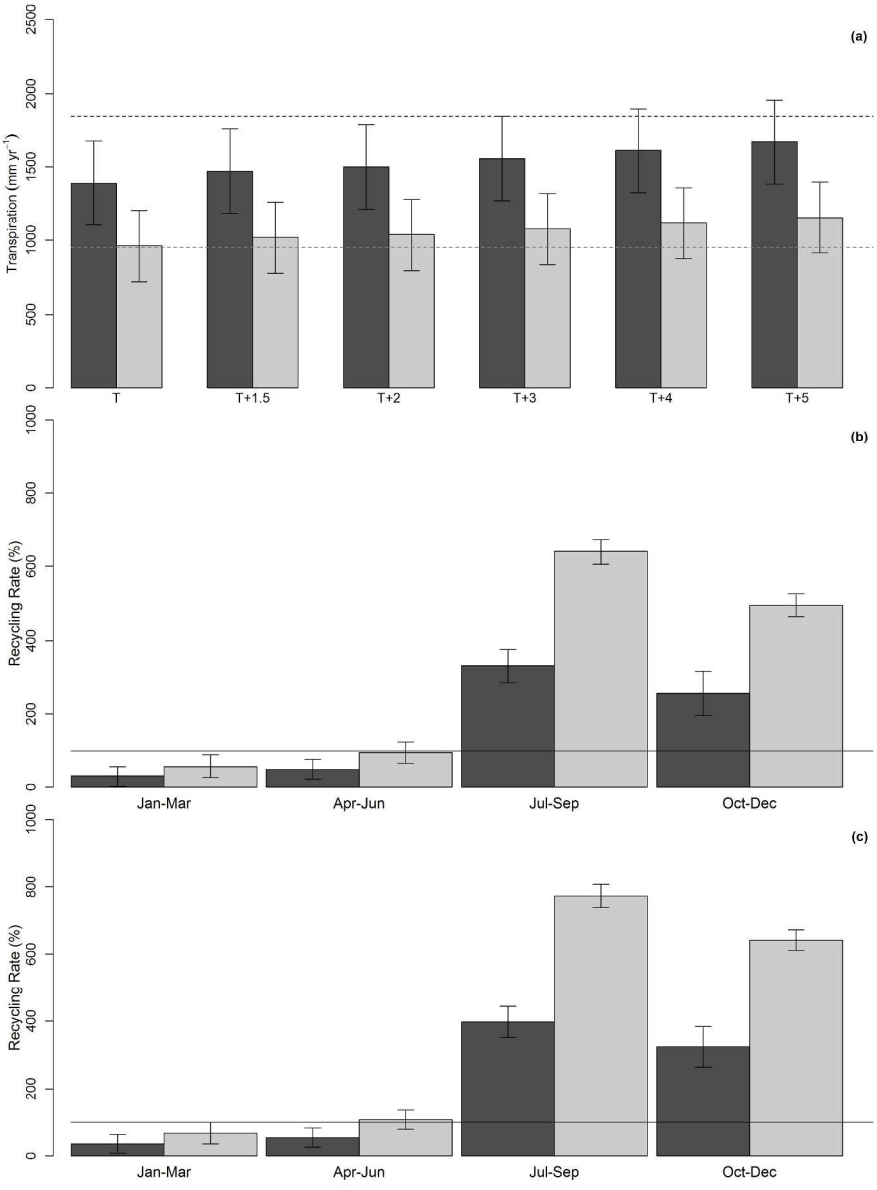

Figure 6: The effect of increasing temperature on annual transpiration fluxes for control (C) and TFE (a.), under current temperature climate (T, year 2015 used) and under the climate of this year + 1.5, 2, 3, 4, and 5°C, accounting for temperature-driven changes in relative humidity and vapour pressure deficit. Dashed lines (a.) indicate the rainfall reaching the forest floor on control (black) and TFE (grey). Rainfall reaching the forest floor is estimated from rainfall minus a canopy interception estimate of 21.5% (see Methods). Panel b. and c. show the % of seasonal through-fall recycled as transpiration during the four quarters of the year, under the current climate (b.) and with a 5 °C increase in temperature (c.). Solid lines in b. and c. indicate 100%, where transpiration exceeds the rainfall reaching the soil. Error bars show the standard deviation across the 100 estimates made of each scenario (see Methods).

304x381mm (300 x 300 DPI)